International Food Research Journal 29(3): 659 - 666 (June 2022)
Journal homepage: *http://www.ifrj.upm.edu.my*

Atomisation of nanometre-scaled jasmine flower extracts using electrospray method

[1]Rahmam, S., [1]*Naim, M. N., [2]Bakar, N. F. A. and [1]Mokhtar, M. N.

[1]Department of Process and Food Engineering, Faculty of Engineering, Universiti Putra Malaysia, 43400 UPM Serdang, Selangor, Malaysia
[2]Faculty of Chemical Engineering, Universiti Teknologi MARA, 40450 Shah Alam, Selangor, Malaysia

Article history

Received:
6 May 2019
Received in revised form:
5 April 2021
Accepted:
14 October 2021

Keywords

Coulomb fission, electrospray, evaporation rate, droplet fission, solidification

Abstract

The present work demonstrated the application of a non-thermal technique to solidify nanometre-scaled atomised droplet using electrostatic atomiser or electrospray. The droplets were prepared in an aqueous solution, and consisted of bioactive compounds extracted from jasmine flower. The jasmine flower extracts were electrosprayed at various concentrations of 5, 15, and 25 wt%, with the working distances between the needle's tip to an aluminium collector being 10, 20, and 30 cm. During the process, the water evaporation rate decreased from 2.02 to 1.02 nm^3/s when the distance was increased from 10 to 30 cm at 5 wt% concentration. The same decreasing evaporation rate pattern was also observed when the concentration was increased from 5 to 25 wt%. On the contrary, increasing droplet fission numbers were observed as the distance was increased from 10 to 30 cm (*i.e.*, from 7 to 406 at 25 wt% concentration) due to the electrostatic charge increment per unit area as the water left the droplet surface. Therefore, water evaporation and droplet fission number are important for solidifying the compounds when the droplets have exceeded their Rayleigh limit.

Introduction

Bioactive compounds from jasmine flower produce rejuvenating aroma, and are commonly used in food industries as flavour and fragrance. The application of non-thermal technique for solidifying bioactive compounds from jasmine flower extracts is practical as compared to the thermal-assisting technique, *i.e.*, spray drying, due to the heat sensitivity issue that affects the degradation of the bioactive compounds. Furthermore, jasmine flower extracts in liquid form are also not preferable over the solid form due to handling issues, especially in cost, transportation, and storage. Therefore, solidifying bioactive compounds with minimal thermal-assisted process is necessary to minimise operational costs and increase product quality.

Electrostatic atomiser, or electrospray, is a non-thermal atomisation tool which exerts a strong electric field that applies the formation of Taylor cone and breaks into a stream of droplets when the surface charge is equal to the surface tension of the solution (Kessler and Merril, 2019). A droplet containing an excess of positive or negative charge detaches from its tips and moves through the atmosphere. When a high electric field with small currents is accumulated in the liquid droplet, an electrostatic force is generated at droplet vicinity known as Coulomb force. This Coulomb force competes with the liquid molecules cohesive force in the droplet until the Coulomb force overcomes the molecules' cohesive force. This condition causes the water capillary to deform, and form the Taylor cone (Jaworek, 2008). When the solution that comprises Taylor cone reaches Rayleigh limit (at the point where Coulombic repulsion at the surface charge is equal to the surface tension of solution), the droplets containing an excessive amount of electrostatic charge will jet out (Cech and Enke, 2002). The ejections of smaller droplets from primary droplets reduce the charge without significantly reducing their mass (Bock *et al.*, 2012). The benefit of applying Taylor cone mode along the atomisation process is that it allows the generation of monodispersed particles with narrow size distribution (Saallah, 2014). During electrospraying, evaporation and droplet fission occur simultaneously until the droplets solidify and deposit onto the grounded conductive substrate. The phenomenon occurs continuously as the charged atomised droplet exceeds the Raleigh limit, and

*Corresponding author.
Email: mohdnazli@upm.edu.my
DOI:
https://doi.org/10.47836/ifrj.29.3.17

governs repeated droplet fission (Hiraoka, 2010). Droplet fission cannot happen without liquid evaporation, which causes droplet shrinkage and increases the droplet body's electrostatic charge concentration. The droplet's shrinkage is due to the droplet body's water removal that increases the positive/negative charge concentration until the value reaches the Rayleigh limit (Ahadi and Konermann, 2012).

Electrospraying can be conducted at room temperature and atmospheric pressure, and no further drying step is required since particles' solidification occurs instantaneously (Zhang *et al*., 2019). When the solution is atomised to the gas phase through electrospraying, it undergoes the production of charged droplets from repeated solvent evaporation and droplet disintegration until the production of microscopic particles (Banerjee and Mazumdar, 2012). The evaporation of solvent during flight is one factor that controls the size and shape of the product (Chakraborty *et al*., 2009).

The principal of evaporation rate and droplet fission for solidification via electrospraying has been commonly discussed in many research, but the influence of evaporation rate and droplet fission to the solidified organic compounds have not been comprehensively studied. Therefore, the present work aimed to demonstrate and understand how evaporation rate and droplet fission affect the solidification of bioactive compounds extracted from jasmine flower.

Materials and methods

Materials

Jasmine (*Jasminum grandiflorum* L.) flowers were collected from the garden area of Universiti Putra Malaysia, Selangor, Malaysia.

Sample preparation

Bioactive compounds were extracted from jasmine flowers by using ultrasonic assisted extraction (UAE). Three grams of the flower was uniformly cut and placed in a clean beaker. Sixty millilitre of deionised water (DI) was poured into the beaker, and sonicated. Following sonication, the jasmine flower extracts were centrifuged (10,000 rpm, 20°C, 30 min) to obtain a uniform particle size, and only fine fragment particles in the supernatant layer were collected. The supernatant was rotary-evaporated at 60°C to concentrate the samples. Following rotary evaporation, the concentrates were classified into three samples namely 5, 15, and 25 wt% jasmine flower extracts.

Electrospray

The electrospray setup consisted of a positive charge electrostatic generator, 25 mL plastic syringe, stainless needle, and a syringe pump. The droplet collector or the substrate consisted of a retort stand, aluminium substrate, a ring electrode, and a negative charge power supply. The experimental setup illustration was referred from our previous work (Rahmam *et al*., 2016).

In the present work, the same electrospray conditions were applied to 5, 15, and 25 wt% jasmine flower extracts. The applied voltage was 4 - 4.5 kV, and the flow rate was 0.2 mL/h. The distance between the tip to the aluminium collector was varied to 10, 20, and 30 cm, and the completion of the electrospray took about 6 h. The collection of solidified particles was collected in batches (not continuously) at 10, 20, 30 cm.

Total water removal

Evaporation of solvent occurred at the droplet interfacial layer along the trajectory path towards the collecting plate. The volume difference between the initial and final droplets was considered as the volume of water removal. This volume had the same amount of water that had been evaporated during electrospraying. The total evaporation rate removed from the initial wet droplet to the final particle size was calculated using Eq. 1:

$$E_r = \frac{\Delta V}{t} \quad \text{(Eq. 1)}$$

where, ΔV = volume difference between the initial droplet and final particles (nm^3); t = time taken for the droplets to reach collector (s); and Er = evaporation rate (nm^3/s).

Besides that, the amount of water removal due to the relative humidity (RH) was also evaluated. The experiment was conducted at a constant room temperature of 20°C, and the initial humidity of 38 - 40%. The amount of moisture removed (ΔY) was obtained from the psychrometric chart by referring to the final condition of RH, and temperature after electrospraying concluded. The final RH values for all samples are tabulated in Table 1.

Table 1. Final RH (RH_{fin}) values for 5, 15, and 25 wt% jasmine flower extracts vary with different collection distances.

Distance (from needle tip to collector, cm)	RH_{fin} of 5 wt% jasmine extract	RH_{fin} of 15 wt% jasmine extract	RH_{fin} of 25 wt% jasmine extract
10	57 ± 2	59 ± 1	60 ± 2
20	66 ± 1	67 ± 2	69 ± 1
30	73 ± 2	75 ± 2	80 ± 2

In order to determine the value of water removal in kg/s (dw/dt), Eq. 2 of the evaporation rate was applied (Earle, 2013). The obtained value was in nm^3/s, and converted to kg/s by using the water density:

$$\frac{d_w}{d_t} = kA\Delta Y \quad \text{(Eq. 2)}$$

where, dw/dt = mass being transferred (kg/s); k = mass transfer coefficient (kg/m^2s; the coefficient varied based on the samples used); A = area of droplet through which the transfer was taking place (nm^2); and ΔY = humidity difference (kg/kg).

Droplet fission

The droplet fission was calculated to determine the quantity of droplet disintegration. As the droplet fission increased, the particle size at the collector decreased. The droplet fission was calculated based on the ratio of droplet's volume over particles' volume (with the assumption that the droplets were in a spherical shape) as described in Eq. 3 (Zolkepali *et al*., 2016). The droplet's volume was initially obtained from the calculation of size using Hartman's equation.

$$d_d = \left(\frac{\rho\varepsilon_o Q^3}{\gamma K}\right)^{1/6} \quad \text{(Eq. 3)}$$

where, d_d, $\rho, \varepsilon_o, Q, \gamma$, and K = size of droplet (nm), density of solution (kg/m^3), electrical permittivity of the vacuum (8.8×10^{-12} $C^2/N/m^2$), flow rate of solution (m^3/s), surface tension, and electrical conductivity, respectively.

The droplet size was converted to the volume of droplet using the volume of the sphere equation. Meanwhile, the particle size obtained from SEM images was converted to the volume of particles by using the sphere equation's volume.

$$d_f = \left(\frac{V_d}{V_p}\right)^3 \quad \text{(Eq. 4)}$$

where, d_f, V_d, and V_p = droplet fission, volume of droplet, and volume of particles, respectively. This equation can be simplified to Eqs. 5 and 6:

$$df = [(4/3)\pi r_d^3] / [(4/3)\pi r_p^3] \quad \text{(Eq. 5)}$$

$$d_f = r_d^3 / r_p^3 \quad \text{(Eq. 6)}$$

where, r_d^3 and r_p^3 = radius of droplet and particles, respectively.

Scanning electron microscopy (SEM)

The morphology of the collected particles was observed using SEM (JSM 6510, JEOL, Tokyo) at the accelerating voltage of 10 - 20 kV and magnification of 20,000×. To avoid the charging effect during SEM observation, all samples were sputter-coated with gold (JFC 1200, JEOL, Tokyo) under vacuum conditions.

Results and discussion

Solidification of bioactive compounds from the jasmine flower extracts consisted of two main mechanisms which are solvent evaporation and droplet fission. For verification purposes, the evaporation rate was estimated by referring to the water removal available in the psychrometric chart. The sample was varied at the specific concentrations and distances to determine the relationship between the evaporation rate and droplet fission. The evaporation rate values are tabulated in Table 2, while the droplet fission values are tabulated in Table 3.

Using Eq. 1, it can be understood that the droplet evaporation rate was influenced by two main factors which were volume differences and time taken for the droplets to reach the collector. The volume difference between the initial droplet and deposited particles at the collector (final particles) can be assumed as the amount of water being removed during electrospraying. From Table 2, the volume difference increased as the distances were increased

from 10 to 30 cm, which indicated the accumulation amount of water that had been removed by evaporation. The evaporation rate was calculated based on the distances and concentrations from the obtained volume differences representing the total amount of water removal. Therefore, the decreasing trends in Figure 1 could be due to these values.

Table 2. Evaporation rate and water removal for 5, 15, and 25 wt% jasmine flower extracts vary with different collection distances.

Parameter	5 wt% jasmine extract			15 wt% jasmine extract			25 wt% jasmine extract		
Distance (cm)	10	20	30	10	20	30	10	20	30
Volume difference, ΔV (× 10^8 nm^3)	2.60	3.71	3.94	2.28	3.26	3.47	1.96	2.79	2.98
Time taken, t (s)	0.12	0.23	0.35	0.11	0.22	0.32	0.1	0.19	0.29
Evaporation rate, Er (× 10^9 nm^3/s)	2.17	1.61	1.13	2.07	1.48	1.08	1.96	1.47	1.03
Water removal, dw/dt (× 10^{-13} kg/s)	2.22	1.58	1.13	2.12	1.51	1.07	2.02	1.44	1.02

Table 3. Droplet fission and electrical conductivity for 5, 15, and 25 wt% jasmine flower extracts vary with different collection distances. Fission number and mean solidified particles were obtained from SEM images.

Parameter	5 wt% jasmine extract			15 wt% jasmine extract			25 wt% jasmine extract		
Distance (cm)	10	20	30	10	20	30	10	20	30
Fission number	5	16	203	6	17	296	7	19	406
Mean particles size (nm)	538 ± 22	364 ± 19	155 ± 19	490 ± 32	339 ± 18	131 ± 13	440 ± 21	312 ± 20	112 ± 15
Initial droplet (nm)		911			873			829	
Electrical conductivity (S/m)		0.042			0.060			0.085	

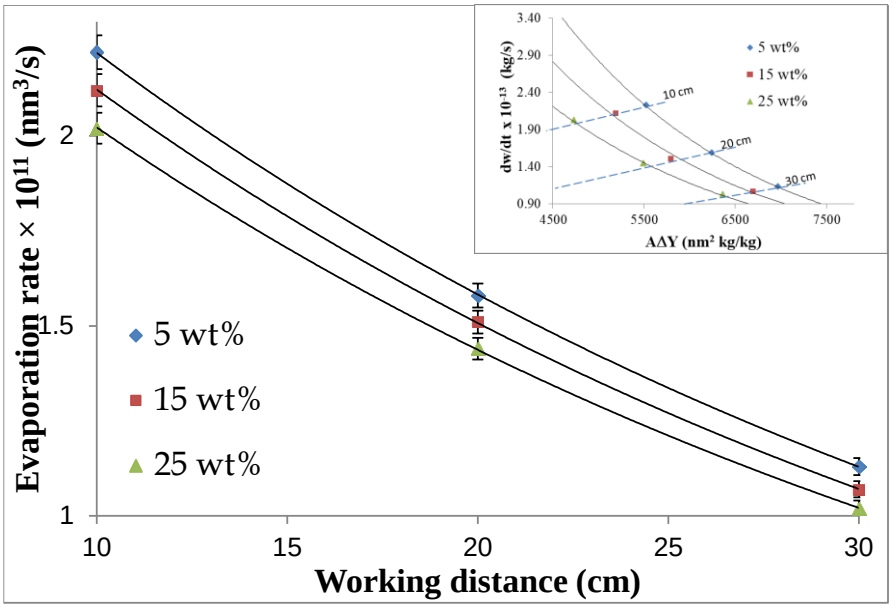

Figure 1. Total water removal for 5, 15, and 25 wt% jasmine flower extracts from 10 to 30 cm distance, calculated using Eq. 1. Graph insert indicates the decreasing solvent evaporation rate vs RH, calculated using Eq. 2.

Figure 1 shows the decrease in droplet evaporation rates against the working distance. From this result, it was noticed that the dependent parameter that controlled the evaporation rate of the jasmine flower extracts was the working distance, and less influenced by the concentration. The obtained values also agreed with the theoretical evaporation principles. As the water molecules at the water-gas

interface are gradually removed, the remaining water molecules inside the droplet would be bound stronger and tighter as its quantity decreases (Earle, 2013). Therefore, when the droplet travels in a longer distance, the droplet's moisture and water content decrease, thus decreasing the water evaporation rate. That condition also indicated that hydrogen bonding attraction forces between water molecules and the compounds were less attractive at low jasmine flower extract concentrations. The bond became stronger when the droplets' volume decreased due to water losses during evaporation. This condition allowed for the release of water from droplet rapidly, with the rate about 2.17 × 109 nm^3/s initially, but decreasing to 1.13 × 109 nm^3/s, in the case of 5 wt% concentration. Similar decreasing patterns were also observed for 15 and 25 wt%, respectively. Since the electrospray system was conducted in a closed chamber, the evaporated water molecules travelled to the surrounding air, and increased the surrounding relative humidity (RH). Therefore, longer working distance led to higher RH as compared to initial.

As the evaporation rate involved RH, a graph that represents the relationship between water removal and humidity is illustrated in Figure 1. The water removal is represented by the small insert in Figure 1 by plotting dw/dt against AΔY using Eq. 2. Since the electrospraying was conducted in the close chamber as illustrated in Figure 2, the measurement was conducted by referring to the humidity changes inside the close system. At the same time, the amount of water removal was calculated using the psychrometric chart. Theoretically, water removal increases when the relative humidity is low, and decreases when the relative humidity is high.

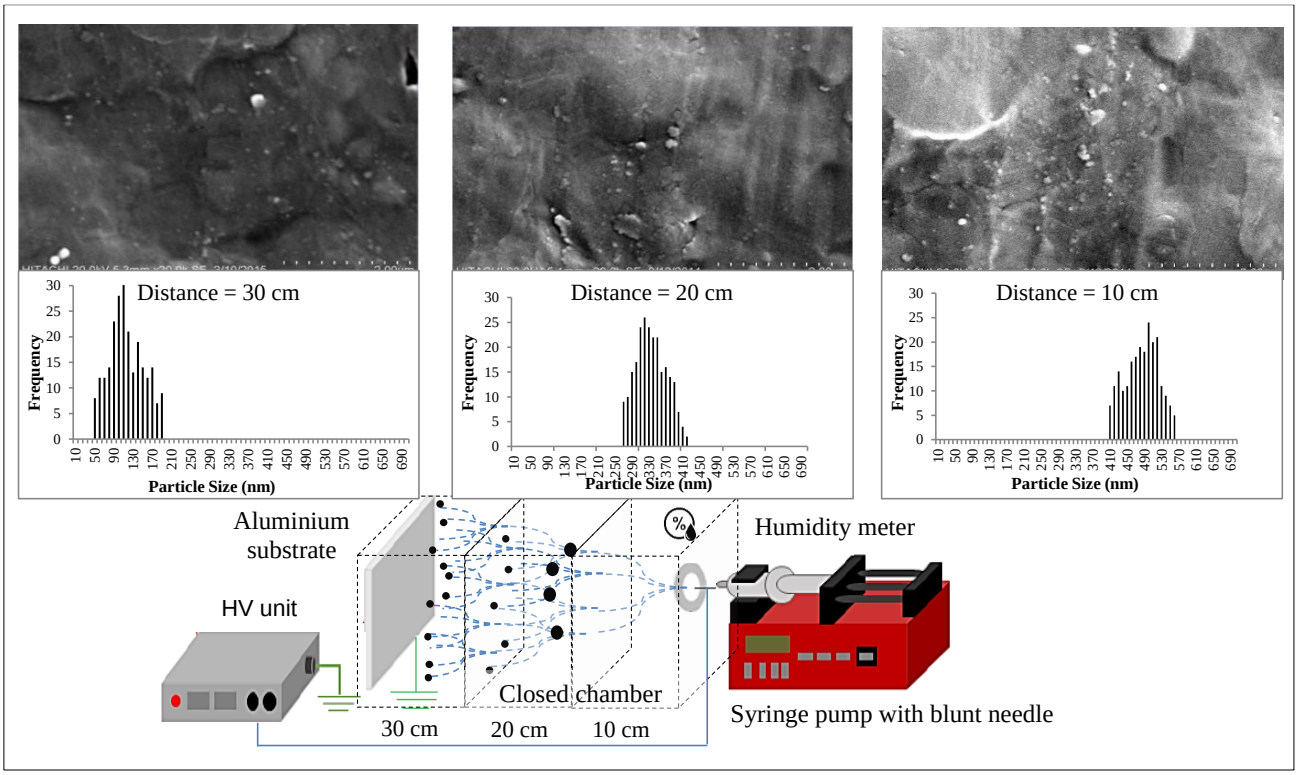

Figure 2. Droplet morphology from SEM images (top); and illustration of droplet evaporation and droplet fission (below).

By referring to Table 2, the 5 wt% jasmine flower extract showed a higher water removal rate as compared to 25 wt% even though the humidity for 5 wt% was higher than 25 wt%. Higher concentration water molecules in 5 wt% contributed to higher humidity value in the chamber than the 25 wt%.

Identification of droplet fission

As compared to normal atomisation droplet, *i.e.*, spray drying, the electro-sprayed atomisation experiences high charge accumulation as the droplet's solvent evaporates. When the charge accumulation of individual droplet increases and surpasses the Rayleigh limit, the occurrences of droplet fission increase. Therefore, the number of droplet fission in the present work was calculated in order to determine

the quantity of droplet disintegration. Table 3 shows the droplet fission for all samples.

Referring to Table 3, by comparing the distance from 10 to 30 cm at the concentrations of 5, 15, and 25 wt%, the disintegration of droplets from its initial condition increased due to the long travel time and distance for the droplets to reach the collector. This phenomenon was due to the decrease in volume by water molecules evaporation of a highly charged droplet as the distance was increased (Hiraoka, 2010). The evaporation of water increases the surface charge density and repulsion between the surface charges (Scholten *et al*., 2011). High charged droplet formed by electrospraying tends to undergo fission to produce progeny droplets. The droplet fission occurs when the droplet charges approach between 60 to 90% of Rayleigh limits. The droplets become unstable at this condition, and the subsequent Coulombic fission generates progeny droplets that have a significantly smaller size as compared to the initial droplet (Tang and Smith, 2001). Therefore, when the distance between the needle tip and the collector was increased in the present work, more droplet fission occurred and produced smaller size deposits as compared to the shorter distance.

The increased distance from 10 to 30 cm contributed to the smaller particle sizes due to the higher number of droplet fission occurrences, as indicated in Table 3. For example, at 10 and 20 cm working distance and due to the short travel distance, low droplet fission numbers were noticed for all wt% of the jasmine flower extracts. On the contrary, at 30 cm, the droplet fission numbers: mean particle sizes were > 1 for all wt% of the jasmine flower extracts.

Drying mechanism through evaporation and droplet fission

Referring to Figure 1 and Table 3, we concluded that the total water removal consisted of solvent evaporation and droplet fission mechanism which could solidify the atomised droplet during electrospraying. Figure 2 illustrates the relationship between evaporation rate, droplet fission, and the droplet morphology at the collector as obtained from the SEM images.

'Wet' deposition at the shorter distance was due to the incomplete water evaporation and droplet fission. The short distance of electrospray also did not allow the droplets to experience sufficient drying, thus producing wet and aggregated solidified particles.

By referring to Tables 2 and 3, at 25 wt%, the values of evaporation rate, droplet fission, and particles sizes at the distance of 10 cm were 1.96 × 109 × 1011 nm^3/s, 7, and 440 ± 21 nm, respectively; while at 30 cm, the evaporation rate, droplet fission, and particles sizes were 1.03 × 109 nm^3/s, 406, and 112 ±15 nm respectively.

Any increase in distance contributed to the decrease in particle sizes due to a longer distance trajectory that provided more frequency for the droplets to experience enough water evaporation and droplet fission. In addition, smaller particle sizes were produced as the concentration increased due to the solution's conductivity value. Higher electrical conductivity at the higher concentration indicated the solution's ability to conduct more electrical charges flow, and allow for more break-up of droplets through droplet fission.

We also concluded that the droplet fission increased after the evaporation rate decreased, thus resulting in fine and non-aggregate particle sizes. Based on this finding, we also believed that the droplet fission mechanism played a more important role rather than the droplet evaporation during the total water removal. However, its occurrence was slower as compared to the common thermal-assisted drying. Furthermore, a faster evaporation rate was found to limit droplet fission, hence producing bigger particle sizes due to interparticle collision before reaching the substrate or collector. According to Bohr *et al*. (2012), fast compound evaporation will also limit the droplet's fission number due to the faster solidification before reaching the substrate. Figure 2 shows the evaporation rate and droplet fission phenomena for 25 wt% jasmine flower extract at 10 to 30 cm working distances.

Droplet evaporation plays an important role in solidifying the droplets. However, the unique application of electrospray is its ability to solidify the droplets through electrostatic charge, thus making the droplet fission having a more dominant effect in solidifying the droplets. Therefore, with the increase of distance from 10 to 30 cm in the present work, the droplets had a longer trajectory flight and solvent evaporation time, thus providing more time for the Coulombic explosion to occur, and leading to the production of smaller particle sizes (Hazeri *et al*., 2012).

Conclusion

The total water removal during electrospraying consists of droplet evaporation and droplet fission mechanisms that can influence bioactive compounds' solidification. In the present work, however, with the application of electrostatic force during electrospraying, droplet fission was identified to have a more dominant effect on solidification due to the electrostatic charge's ability to repel water molecules under the Rayleigh limit condition, and produce continuous droplet fission which contributed to fine and dry solid particles.

Acknowledgement

The present work was financially supported by Putra Grant GP-IPS/2015/9465200 and GP/2018/9647900, Universiti Putra Malaysia, Serdang, Selangor, Malaysia; and 600-IRMI/MYRA 5/3/BESTARI (021/2017), Universiti Teknologi MARA, Shah Alam, Selangor, Malaysia.

References

Ahadi, E. and Konermann, L. 2012. Modeling the behavior of coarse-grained polymer chains in charged water droplets: implications for the mechanism of electrospray ionization. Journal of Physical Chemistry 116(1): 104-112.

Banerjee, S. and Mazumdar, S. 2012. Electrospray ionization mass spectrometry: a technique to access the information beyond the molecular weight of the analyte. International Journal of Analytical Chemistry 2012: article ID 282574.

Bock, N., Dargaville, T. R. and Woodruff, M. A. 2012. Electrospraying of polymers with therapeutic molecules: state of the art. Progress in Polymer Science 37(11): 1510-1551.

Bohr, A., Yang, M., Baldursdottir, S., Kristensen, J., Dyas, M., Stride, E. and Edirisinghe, M. 2012. Particle formation and characteristics of Celecoxib-loaded poly(lactic-co-glycolic acid) microparticles prepared in different solvents using electrospray. Polymer 53(15): 3220-3229.

Cech, N. B. and Enke, C. G. 2002. Practical implications of some recent studies in electrospray ionization fundamentals. Mass Spectrometry Reviews 20(6): 362-387.

Chakraborty, S., Liao. I., Adler, A. and Leong, K. W. 2009. Electrohydrodynamics: a facile technique to fabricate drug delivery systems. Advanced Drug Delivery Reviews 61(12): 1043-1054

Earle, R. L. 2013. Drying rate. In Earle, R. L. (ed). Unit Operation in Food Processing, p. 95. New Zealand: NZIFST Inc.

Hazeri, N., Tavanai, H. and Moradi, A. R. 2012. Production and properties of electrosprayed sericin nanopowder. Science and Technology of Advanced Materials 13(3): article ID 035010.

Hiraoka, K. 2010. Fundamentals of mass spectrometry - fundamentals of electrospray. Journal of the Mass Spectrometry Society of Japan 58: 139-154.

Jaworek, A. 2008. Electrostatic micro- and nanoencapsulation and electroemulsification: a brief review. Journal of Microencapsulation 25(7): 443-468.

Kessler, D. A. and Merrill, M. 2019. A Lagrangian-Eulerian method for simulating electrospray deposition. United States: American Institute of Aeronautics and Astronautics (AIAA).

Rahmam, S., Naim, M. N., Ng, E., Mokhtar, M. N. and Bakar, N. F. A. 2016. Encapsulation of bioactive compound from extracted jasmine flower using β-cyclodextrin via electrospray. IOP Conference Series Earth and Environmental Science 36: article ID 012054.

Saallah, S. 2014. Immobilization of cyclodextrin glucanotransferase on electrospun polyvinyl alcohol nanofibers. Malaysia: Universiti Putra Malaysia, MSc thesis.

Scholten, E., Dhamankar, H., Bromberg, L., Rutledge, G. C. and Hatton, T. A. 2011. Electrospray as a tool for drug micro- and nanoparticle patterning. Langmuir 27(11): 6683-6688.

Tang, K. and Smith, R. D. 2001. Physical/chemical separations in the break-up of highly charged droplets from electrosprays. Journal of the American Society for Mass Spectrometry 12(3): 343-347.

Zhang, S., Campagne, C. and Salaun, F. 2019. Influence of solvent selection in the electrospraying process of polycaprolactone. Applied Sciences 9(3): article no. 402.

Zolkepali, N. K., Bakar, N. F. A., Naim, M. N., Anuar, N., Aripin, N. F. K., Bakar, M. R. A., ...

and Kamiya, H. 2016. Formation of fine and encapsulated mefenamic acid form I particles for dissolution improvement via electrospray method. Particulate Science and Technology 36(3): 298-307.